Title: Unbound states of neutron-rich isotopes via direct reactions

Spokesperson(s) *(max. 3 names, laboratory, e-mail - please underline among them one corresponding spokesperson):*
V. Lapoux, **CEA-Saclay, DSM/DAPNIA/SPhN**, vlapoux@cea.fr

GANIL contact person
P. Roussel-Chomaz

Collaboration *(names and laboratories):*

CEA-Saclay, DSM/DAPNIA/SPhN France: N. Alamanos, F. Auger, R. Dayras, A. Drouart, A. Gillibert, N. Keeley, V. Lapoux, X. Mougeot, L. Nalpas, E. Pollacco, C. Simenel
GANIL, France: W. Mittig, F. de Oliveira, L. Gaudefroy, P. Roussel-Chomaz, O. Sorlin, H. Savajols
IPN-Orsay, France: D. Beaumel, S. Fortier, F. Hammache, E. Khan, C. Petrache
HMI Berlin, Germany: H.G. Bohlen, Tz. Kokolova, W. Von Oertzen, C. Wheldon
IKS University of Leuven, Belgium: R. Raabe
JINR, FLNR Dubna, Russia: A. Fomichev, G Golovkov , A. Rodin, S. Sidorchuk, S. Stepantsov, G. Ter-Akopian, R. Wolski
IPHC Université Louis Pasteur, Strasbourg: Ch. Beck, S. Courtin, A. Khouaja
INFN-Catania, Italy: A. Musumarra
KVI, Netherlands: M.N. Harakeh, H.G. Wortche
Florida State University, USA: K. Kemper
University of Huelva, Spain: I. Martel
University of Ioannina, Greece: T.J. Merzimekis, A. Pakou, D. Roubos
University of Santiago de Compostela, Spain: M.D Cortina-Gil

Theoretical support:

CEA-Saclay, DAM/DIF/DPTA/SPN, Bruyères-le-Châtel, France: E. Bauge, P. Chau Huu-Tai, J.P. Delaroche, H. Goutte, S. Péru-Desenfants
CENBG Bordeaux: M. Bender
IST Lisboa, Portugal: R. Crespo
IPN Lyon: K. Bennaceur
The A. Soltan Institute for Nuclear Studies, Hoza, Warsaw, **Poland:** K. Rusek
NSCL, MSU, USA: T. Duguet
University of Pisa-INFN-Pisa: G. Blanchon, A. Bonnacorso
The Open University, UK: R.S. Mackintosh
University of Sevilla, Spain: A.M. Moro
VAEC Hanoï, Vietnam: Dao. T. Khoa; **INST Hanoï:** Hoang S. Than

Abstract:

The objectives of our program with the new beams are to extend the exploration of the shell structure and the shell gaps as far as possible from the valley of stability, at large isospin and at the limits of nuclear binding, in order to confront the most advanced microscopic predictions to our experimental results and analysis. We want to investigate the profiles of the transition densities to the bound and also to the unbound states, to study the evolution of the neutron excitation along isotopic chains, like e.g. Ni, Kr, Sn, and inspect the behaviour of the neutrons in the vicinity of the expected neutron shell gaps.

The evolution of the neutron excitation will be determined through proton inelastic scattering experiments, and the neutron transfer reactions like (p,d) or (d,p) will fix the single-particle picture and the shell gaps in the neighbourhood of the expected new doubly-magic nuclei.

The more neutron-rich nuclei produced by the SPIRAL2 beams will be weakly-bound, with few or no bound excited states, and couplings to the continuum are expected to play a significant role since the scattering states are much closer to the continuum states than in stable nuclei. To disentangle the structure from reactions, and obtain the features of the unbound states, we will develop a program to carry out and analyze coupled-channel reactions (elastic, inelastic, transfer) on proton or deuteron targets.

This letter of intent will develop a part of the physics cases addressed by the LOI "GASPARD-Direct reaction studies at SPIRAL2". *It will combine light particle spectroscopy in a telescope device in coincidence with the identification of the heavy fragment at forward angle in a spectrometer, like SPEG or VAMOS.*
An important asset of the experimental technique is the access to both bound and unbound excited states through the kinematical reconstruction of the reaction from the light particle detection and missing mass method. In case of a high level-density of bound excited states in the exit channel, the gamma-rays will be measured in coincidence by a gamma spectrometer.
The principles of such experiments and the detection requirement will be explained.

Scientific case

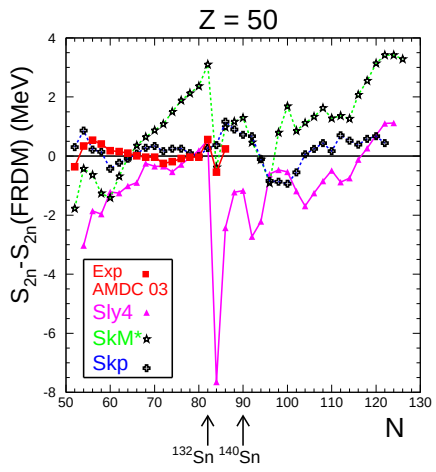

Fig1. Differences between two-neutron separation energies (S_{2n}) calculated with the finite-range droplet model (FRDM) and measured values for the tin isotopes (from [AMDC]). The differences between FRDM and the predictions from the HFB model assuming various parame-trizations of NN effective interactions (Sly4, SkM, SkP) are shown by the curves. The calculations are explained in [Sto03].*

In order to test the validity of the nuclear models, and to improve their predictive power, the new properties of the exotic nuclei are experimentally investigated using the radioactive ion beams. The effective nuclear interaction far away from stability and its dependence on the proton-to-neutron ratio is not well known. For instance, the theoretical predictions diverge on the structure and spectroscopic properties of the very neutron-rich nuclei and the discrepancies are peculiarly important as the isospin increases (Fig.1). Experimental studies are needed to determine:

- The structure of nuclei at the drip lines and the development of the shell structure in nuclei with a large proton-neutron asymmetry with respect to stable isotopes;
- The evolution of the proton and neutron excitations as a function of the isospin degree of freedom.

Shell structure and modifications far away from the valley of stability

The magic numbers are key-stones for the modelling of the nuclear structure and the understanding of the nuclear properties. For instance, the values of a few shell gaps energy between single-particle states and the charge root mean square (rms) radii for the doubly-magic nuclei (^{16}O, ^{208}Pb) are key values to fix the parameters of the effective Nucleon-Nucleon (*NN)* interactions like Skyrme-type [Cha95] and Gogny-D1S type interactions [Dec80] used in the mean-field and beyond mean-field Hartree-Fock-Bogolyubov (HFB) calculations. Within the shell model, the magic nuclei represent the building block of the effective core interaction [ChW92].
The ground structure properties of ^{132}Sn were taken into account in the Skyrme parametrization, along with the ones of other doubly closed-shell nuclei [Cha97]. It is expected that the new properties of the unstable nuclei in the intermediate mass region could provide a more realistic estimation of the effective *NN* interaction, better adapted for the calculation of the equation of state of the neutron-rich matter and for the neutron star densities. Recently a new relativistic mean-field effective interaction with explicit density dependence of the meson-nucleon couplings was adjusted, taking into account properties of doubly-closed shell nuclei, among which ^{132}Sn [Lal05].

With the few parameters adjusted on the properties of the doubly-closed shell nuclei the nuclear forces were found to give a satisfactory description of the stable nuclei. But the validity of the present theories to describe the radioactive nuclei has been put under question.
The first-generation of RIBs beams around the world, and in particular the SPIRAL1 facility, has opened a first window on the nuclear chart and provided data on the light unstable nuclei. The important learning was the modification of the usual shell structure established for the stable nuclei. Today, the location of the neutron drip line is known only up to the oxygen isotopes; the last bound nucleus being ^{24}O (N=16) and not the expected doubly-magic nucleus ^{28}O (N=20). New magic numbers have been indicated experimentally, like N=16 for C, N, O isotopes [Oza00]; new shell effects around N=16 for ^{26,27}Ne [Obe06] and the shell effects associated to the well-known magic numbers like N=20 were shown to vanish in the neutron-rich nuclei like the deformed ^{32}Mg nucleus.

The new N=16 magic number was interpreted [Ots01,Ots03] as the effects of the tensor proton-neutron tensor force, producing an enhancement of the neutron shell gap between the s1/2 and the d3/2 subshells, as compared to the situation of the *sd* shell in the stable nuclei.

Recently, T. Otsuka et al., have discussed the general rules for the evolution of the Effective Single Particle Energies (ESPE) [Ots05] and found that the movement of the ESPE (repulsive or attractive effects between orbitals) was driven by the proton-neutron tensor force. Along the isotonic or isotopic chains, moving towards the drip-lines, the spherical single-particle energies are shifted as protons or neutrons occupy certain orbits.

In the model beyond-mean field using Gogny forces, HFB calculations have exhibited shell modifications but the evolution of the shell gaps is less pronounced [Obe05]. Recently RMF calculations have explored the change of the spin-orbit term for neutron-rich nuclei [Tod04]. The spin-orbit potential may be strongly different from what was usually assumed for the stable nuclei.
Isovector force, pairing correlations, isospin-dependence of the interaction terms are not well determined in this procedure since the sample of nuclei in the valley of stability, offers a too narrow range for the variation of the isospin degree of freedom. This is one of the reasons why the present parameterizations are failing in reproducing the nuclear data collected up to now in the case of the exotic nuclei. Another cause for the observed discrepancy is attributed to the role played by the continuum correlations, which were found to be enhanced when the nuclei are getting more and more weakly-bound, which is the case, going to the drip-lines.

The models have to take into account two main ingredients to improve their predictive power over the whole nuclear chart:
- The effect of the continuum to continuum states, which may become predominant for weakly-bound systems with low particle threshold, which is the case for nuclei close to the drip-lines,
- The correct dependence of the nuclear forces with the isospin degree of freedom, along with the modification of the spin-orbit term and of the pairing correlations for unstable nuclei.

To determine these modifications and to test the features of the renewed nuclear models, we need to explore the change of the nuclear shell properties at higher isospin when going far from the valley of stability. **The radioactive nuclei associated to usual magic proton and neutron numbers, like Z=28, N=20,28,50 ^{48,56,78}Ni, and Z=50,N=50,82 ^{100,132}Sn will complete the set of the few key double-magic nuclei known in the valley of stability, ^{4}He, ^{16}O, ^{40,48}Ca, ^{208}Pb.**
These regions are not the only ones to consider for the exploration of the single-particle properties. Far away from the valley of stability the shell structure is predicted to be modified in terms of a weakening of the long-known magic numbers and the possible appearance of new shell gaps. For instance, it has been suggested that the harmonic oscillator shell gaps should become relevant when approaching the neutron drip-line.
For medium-mass nuclei far away from stability the shell gaps at Z=28; N, Z=50, and N=82 are predicted to be weakened, and new gaps are expected to appear at N, Z=40, 70 when approaching the neutron drip line. The magic shell properties are becoming local properties in the nuclear chart, which means that **we need to lead systematic investigation of the proton and neutron shell effects as a function of the proton number, and along extended isotopic chains.**

As neutron-proton difference is increasing, the decrease of the binding energies and structural changes (surface diffuseness of the nuclei) are observed, and can be theoretically attributed to the combined effects of the spin-orbit force and isospin-dependent terms. On top of these changes, the continuum coupling effects, increased in the weakly-bound systems, produce

also the softening of the nuclear potential resulting in a more diffuse Wood-Saxon potential [Dob95], responsible for a change in the expected neutron gaps.
Several combined effects can produce a modification of the shell structure when going to the neutron drip-line, they must be examined through various structure models, in order to compare the assumptions made on the evolution of the isospin-dependent terms, and in particular to determine the changes introduced by the monopole tensor force, and the spin-orbit interaction. In order to decipher the origin of the change, we need to extend our knowledge on the shell effects in the neutron-rich region, for intermediate-mass nuclei.
In the region of masses greater than 100, ^{132}Sn is the only other doubly-magic nucleus with the stable ^{208}Pb. It will be the core to study the single-particle excitation and will be used as reference nucleus to understand the behaviour of the surrounding nuclei.

The simplest excitations in the doubly-closed shell nuclei consist of particle-hole (p-h) states in which the particles are excited across the energy gap defining the closed shell. **The nuclear shell effects are revealed by the identification of the single-particle (-hole) and 2-particle (-hole) states and by the determination of their spectroscopic factors.** The location of such states is particularly interesting in the region near closed-shell nuclei. The spectroscopic information deduced on the various isotopic chains for neutron-rich unstable nuclei around the Z=50, N=82 will be used to reconstruct the single-particle spectrum for neutrons and protons in this region.

Evolution of the neutron excitation in the regions of large deformation.
The neutron-rich $_{34}$Se and $_{36}$Kr isotopes are predicted to develop a large deformation in the neutron-rich region (N>48) within HFB calculations, performed either with the Skyrme forces [Sto03] or with the Gogny-D1S (BIII calculations). The (p,p') reactions with the SPIRAL2 beams of Se and Kr will give a direct access to the evolution of the neutron excitation up to N= 60.

Astrophysical considerations
The modifications of the shell structure have a strong influence on the modelling of the astrophysical processes: a shell quenching at N=82 (i.e. a shell gap less pronounced than expected through macroscopic-microscopic mass models), and along N=50 and 82 will modify the expected abundances of heavy nuclei.
The structure and spectroscopic information for the unstable neutron-rich nuclei are required as inputs for the r-process calculations (e.g. solar abundances, neutron-capture rates).
See the LOI "r-process nucleosynthesis" which explains the key parameters for the r-process.

Specificity of our studies

An important aspect to be raised is the specificity of our present studies in the international context of the experiments undertaken using the RIBs.
The regions of the new radioactive doubly-magic nuclei will be opened for exploration by the new facilities around the world. For instance, the possible new ^{110}Zr is refractive element will not be produced by the ISOL technique; it will be available at fragmentation facilities like FAIR. FAIR like SPIRAL2 will provide access in the vicinity of possible doubly-closed shell nuclei, like ^{78}Ni, ^{132}Sn. RIBF at RIKEN will also give access to the regions of the very neutron-rich exotic nuclei. But the information on the single-particle structure will be directly

understood by doing (d,p) at low energies, around 10A MeV. This will not be possible at FAIR or RIBF. These studies at SPIRAL2 will be unique.

Another aspect concerns the excited states which can be populated by the direct reactions.
So far, the studies done on the heavy (A>80) neutron-rich isotopes, deal with the nuclear spectroscopy *below the neutron threshold.* These experiments, for instance on the Tin and Te isotopes at Oak Ridge, or at CERN-ISOLDE, using gamma-spectrometers, are limited to small incident energies and give access only to the low-lying spectroscopy of the nuclei.
More generally, the most neutron-rich nuclei which can be studied using SPIRAL2 beams will have mainly very few bound excited states.
Via the missing mass method we will have access to their unbound excited states and will give new spectroscopic data compared to the studies which have been performed at Oak Ridge and at CERN/ISOLDE on the structure of the neutron-rich nuclei around N~50, 82.

It should be noted that, even if new beams of neutron-rich Sn isotopes are or will be available in other facilities like HRIBF at Oak Ridge, these specific studies, and especially those of unbound states, are not feasible today due to the limited beam intensities.

Methodology

1. Probes

Light-ion induced reactions, proton or deuteron elastic and inelastic scattering, few-nucleon transfer reactions using proton, deuteron, alpha probes, like (d,p), (p,d), have been providing for years spectroscopic data on the stable nuclei. These studies have been extended to unstable nuclei, using radioactive beams. Detailed information on the structure of light exotic nuclei can be deduced from direct reactions:

- Excitation modes of the nucleus and the couplings to the low-lying states, to the continuum, and to other reaction channels, are probed by the inelastic scattering, e.g. (p,p') or (d,d').
- The single-particle shell structure and the overlap of the wave-functions (called spectroscopic factors SF) are studied via nucleon transfer reactions like (p,d), (p,t), and (d,p).

The shell structure and shell gaps will be explored via a joint program of Coulomb excitation (Coulex) and (p,p') reactions. Coulex data will be available with the experimental program foreseen by the Gamma spectroscopy Working group for SPIRAL2, using similar technique as the ones developed for SPIRAL beams. Coulomb excitation provides the proton contribution to the excitation, expressed as the electromagnetic transition strength, B(EL). The (p,p') reaction is sensitive to the neutron and proton contributions to the excitation. The combined information from the (p,p') and the Coulomb excitation measurements will disentangle the proton and neutron contributions, namely the transition matrix elements M_p (for a L=2 transition B(E2) = $|M_p|^2$) and M_n. Measurements along isotopic chains allow to compare the evolution of the M_p and M_n values to the microscopic calculations, and to deduce the underlying shell structure.

2. Previous works and results using particle spectroscopy at GANIL

This technique has been applied using detectors like MUST. With the next-generation device MUST2, the MUST2 collaboration, gathering physicists from CEA-Saclay, GANIL and IPN-Orsay, has developed a program of direct reactions induced by radioactive beams to determine their structure and spectroscopy, and to check the evolution of the proton and neutron excitations and of the shell gaps. The experiments are performed in inverse kinematics where the beam impinges on a target containing the light probe (p, d, or t) and the light recoil is identified in a position-sensitive particle detector such as MUST [MUST] or MUST2 [MUST2] in coincidence with the heavy ejectile detected at forward angles in a plastic scintillator or in a spectrometer, like SPEG or VAMOS.

The following list gives an overview of the recent results obtained by the collaboration on the structure of the light exotic nuclei and on the shell structure exploration far from stability:

- Investigation of the nuclear matter distributions of the weakly-bound neutron-rich isotopes ^{6,8}He. The analysis of ^{6}He(p,p') reaction at 40 MeV/n was in favour with the halo of ^{6}He [Lag01] ; from the direct reactions of the ^{8}He SPIRAL beam at 15.7A.MeV on a proton-rich target, the features of the neutron-skin structure of ^{8}He [Ska05,Ska06] were discussed;
- The neutron excitation in the ^{10}C compared to its mirror nucleus ^{10}Be [Jou05];
- The evolution of the neutron excitation in the O chain, up to ^{22}O in favour of an *N*=14 sub-shell closure [Bec06]
- The evolution of the shell gap at N=28 via the ^{44,46}Ar(d,p)^{45,47}Ar reaction using the Ar SPIRAL beam [Gau06], the analyses indicates a reduction of the spin-orbit splitting at the *N*=28 shell closure.

These promising probes and techniques will be extended, in the same spirit, for the study of heavier neutron-rich nuclei produced using the SPIRAL2 beams.

3. Full program using direct reactions on proton and deuteron targets

The total experimental program will cover the following physics cases:

- **the evolution of the neutron excitation and shell effects with neutron number;**
- **The apparition of the neutron-skin structure for N>82**. with (p,p') reactions to investigate the transition densities to the excited states : ex: **$^{132\text{-}134}$Sn(p,p')**
- **The study of the single-particle picture around doubly closed shell nuclei via (d,p) reactions;** We want to explore the neutron shell gaps at *N*=40,50 in the neighbourhood of the Ni chain, the neutron-rich Tin isotopes in the vicinity of N=82, and the excited states of the neutron-rich isotopes around Z=50, N=82. First investigations will be the shell properties in the vicinity of expected doubly-magic neutron-rich radioactive nuclei (^{78}Ni, ^{132}Sn).

SPIRAL2 beams with intensities greater than 10^4 pps (particles per second) are required to have a complete set of angular distributions for elastic and inelastic scattering, and transfer reactions. Following the SPIRAL2 technical document, in the region of Z=50, N=82, the other beams indicated as "relatively easy beams" to produce are $_{48}$Cd $_{49}$In, $_{51}$Sb, $_{53}$I, $_{54}$Xe.
In the most extreme cases reachable with SPIRAL2, the neutron thresholds are low: e.g. $S_n(^{134}Sn)$ = 3.91(10) MeV, $S_n(^{135}Sn)$ = 2.07(41) MeV, $S_n(^{96}Kr)$=5.07(64) MeV [AMDC].
The investigation of the unbound excited states of these nuclei will be an important part of our experimental program using the particle spectroscopy and the missing mass method. In the following section, we explain the particle spectroscopy technique adapted to

the measurement of both bound and unbound states. In Section 5, we will discuss specifically the physics case around the doubly closed shell nucleus ^{132}Sn.

4. Particle spectroscopy technique

The kinematical reconstruction of the direct reaction is obtained from the light particle detection. The main forward angles in the center of mass frame are covered by detecting the light recoil at backward laboratory angles for (d,p) and at forward angles for (p,d), in an array of position-sensitive telescopes (like MUST2 ref [MUST2]), in coincidence with the heavy fragment identified at forward angle in a spectrometer, like SPEG or VAMOS. Both bound and unbound states are measured with this technique through the missing mass method. In approaching the drip line, the neutron-rich nuclei are more weakly bound, and expected to have only a few or no bound excited states, like the known even-even drip-line nuclei (^{8}He to ^{24}O). For ^{24}O, the neutron threshold is 3.7 MeV and no bound excited state was found in this nucleus [Sta04].
The experimental analysis is based upon the complete reconstruction of the reaction kinematics. The small centre-of-mass angles are obtained from the identification and precise measurement of the light recoils at energies below 5 MeV. This requires a low energy threshold in order to correlate energy and time of flight, which is achieved with MUST2 array.

As a prototype for the transfer reactions to unbound states, with the SPIRAL2 beams, we chose to discuss the required detection set-up for **the example of the (d,p) reactions induced by the neutron-Tin isotopes.** We present the case of the ^{134}Sn(d,p)^{135}Sn to explain the experimental conditions. It is an interesting case to examine: in terms of mass and charge identification of heavy reaction products, the reaction studies will be more difficult in the case of the neutron-rich Tin isotopes than for the region around the Ni isotopes. The energy and angular straggling in the target and in the detection systems are large, due to low incident energies and heavy masses. This aspect is detailed in the ***Appendix B*** (detection constraints for the mass and charge identifications), the straggling in the target is discussed in the section "Targets".

Information on unbound states is only given by the proton detection. However, such a measurement can only be performed with a thin target, and beam intensities of at least few 10^4 pps are required. In the proposed experiment with the (d,p) transfer, this beam intensity will be high enough to provide in a one-week experiment the excited states of the ^{135}Sn nucleus by measuring the cross sections above 1mb/sr (roughly corresponding to the angular range up to 35 deg. in the c.m. frame, as can be seen in the **Fig.5. Appendix A**).
If a CD_2 target is used, the presence of ^{12}C may result in the (^{12}C,^{11}C) transfer which will be well separated, kinematically, from the (d,p) reaction. The Carbon background is suppressed using the coincidence with the spectrometer detection of the heavy reaction product.

In case of a high level-density of excited states in the exit channel, the measurement of gamma rays with a high-resolution gamma spectrometer like EXOGAM, and in the future AGATA, is essential to separate the low-lying bound levels.

5. Discussion of the (d,p) reactions induced by neutron-rich Tin isotopes

Due to the proton shell closure at Z=50, it is natural to assume that the low-lying states of the $_{50}A_N$ tin isotopes can be interpreted in terms of N-50 neutrons moving in the shell model orbitals: 1*g*7/2, 2*d*5/2, 2*d*3/2, 3*s*1/2, and 1*h*11/2 , for N < 82;
and N-82 neutrons in 1h11/2, 2f7/2 3p3/2, 1h9/2, 3p1/2 2f5/2 for 82 ≤ N < 126.

We propose to study first the shell closure N = 82 with the measurement of the level scheme of odd Tin isotopes, namely ^{131}Sn (N=81) and ^{133}Sn (N=83) and also the N=84 excitations with the ^{135}Sn level scheme.
In the past, the level scheme of the stable Tin isotopes was determined through a complete set of reaction data: Coulomb excitation, in beam γ-ray spectroscopy, heavy ions induced reactions, inelastic scattering of protons, deuterons, α particles and one- and two-nucleon transfer reactions like (*d*, *t*), (^{3}He,*n*) (t,p) or (p,t). The compilation gives the list of references and results for such studies [Bla02].
The levels of the neutron-rich Tin isotopes ($^{132-135}$Sn) have been studied by beta-decay studies, mainly at ISOLDE. For instance, levels of ^{132}Sn were given from the experiments of ^{132}In β− decay [Bjo86]. Collectivity and p-h states were observed in ^{132}Sn [Fog95] and in the ^{132}Sn region [Omt95].
Above the neutron threshold, the dipole strength in the $^{130-132}$Sn was measured, with a Coulomb excitation experiment performed with the LAND-FRS facility at GSI. A giant dipole resonance was observed and a "pygmy resonance" (resonance-like structure with neutrons oscillating versus core nucleons) was reported at a lower excitation energy around 10 MeV [Adr05].
The shell model calculations were applied to the N=82 isotones [Wil69]. Recently, developments in theories were driven by the need to understand the new spectroscopic data in the region around ^{132}Sn. The structure around ^{132}Sn was calculated using improved shell model calculations described in [Dea04], the HFB framework with Skyrme interactions [Dob94,Sto03]. Low-lying excitations in ^{132}Sn were explored using relativistic RPA calculations [Paa03]. The 2+ excitations around ^{132}Sn recently reinvestigated using HFB calculations and configuration mixing, to explain the anomalous behaviour of 2+ excitation energies and B(E2) values observed in this region, for Te isotopes [Ter02]. The anomalous effect was attributed to a reduced neutron pairing above N=82. The single particle spectroscopy of ^{132}Sn inferred from experimental data is presented below in Fig.2.

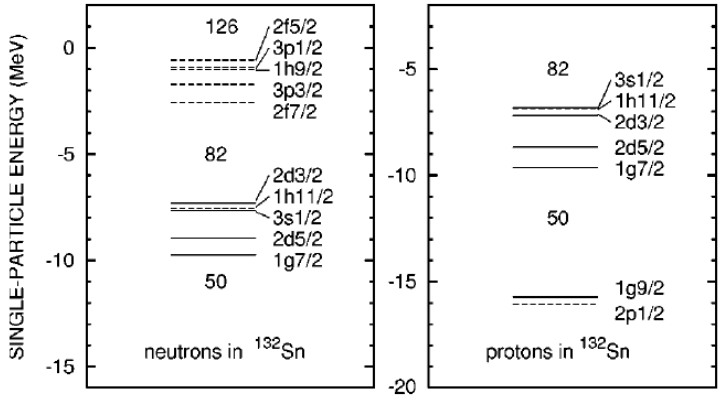

Fig.2 Experimental single-particle spectrum given in [Ter02] (and references therein).

Few transfer data exist for the $^{132-133}$Sn nuclei (HRIBF facility at Oak Ridge) and only the bound states were studied. For ^{133}Sn only the energy of the states was measured, and spin and parities were assumed. For ^{135}Sn, only the ground state was observed. Fig. 3 shows the level

scheme of N = 83, 84, 85 Tin nuclei which can be produced and excited via the (d,p) reactions from the ^{132,133,134}Sn SPIRAL2 beams, respectively.

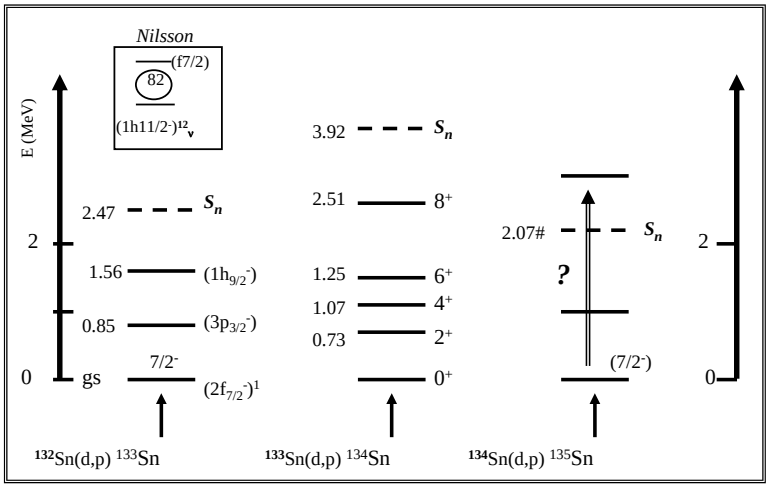

Fig. 3. Low-lying spectroscopy of the ^{133,134,135}Sn isotopes which can be reached by the (d,p) transfer reactions. The known states, below neutron emission threshold, are indicated (from ENSDF data base). According to [AMDC] mass evaluation, the one neutron separation energy in ^{135}Sn is rather low, S_n =2.07 MeV, so that most of these states may be unbound.

Energy domain and criteria of the momentum matching window

The production rates of the one-neutron transfer reactions like (p,d) and (d,p) are favoured in the energy domain between 5 and 20 MeV/n. But it is well known that transfer reactions are very selective as regards all the available states in the final nucleus.

A simple rough estimation of the angular momentum window ΔL which can be reached at a given incident energy can be given by the following classical approximation [Sat83]: ΔL ~kR, where k= k_i -k_f is the transferred momentum, and R the radius associated to the nuclear system of projectile (P) and target (T) R = R_p + R_t = R_o ($A_p^{1/3}$ +$A_t^{1/3}$).

For instance, in the case of the ^{134}Sn(d,p)^{135}Sn reaction done at 5 A.MeV, we obtain ΔL ~2.5 and, at 10 A.MeV, ΔL ~4.

The Nilsson shell gap at N=82 is between ($h_{11/2}$) and ($f_{7/2}$) for $^{132\text{-}135}$Sn, and the expected orbital configuration of single-particle states are: ($f_{7/2}$) ($p_{3/2}$) ($h_{9/2}$) ($p_{1/2}$) ($f_{5/2}$) as inferred from experimental data (see Fig 3) and indicated through HFB calculations [Ter02].

For the ground state of ^{135}Sn the configuration $(f_{7/2})^3$ can be expected, and for the excited states we may have: 7/2-, 3/2-, 9/2-, ½-, 5/2- . From the momentum matching conditions, at 5 A.MeV, with ΔL ~3, the states 5/2-, 7/2- are preferentially populated, while at 10 A.MeV with ΔL ~4 the states 7/2- (gs), 9/2- will have larger cross sections. Complete estimations can be given using coupled-channel calculations of the transfer at 5 and 10 A.MeV with the ECIS code [Ray81], global parametrizations of the entrance and exit potentials, standard spectroscopic factors S_{ij} = 1.

For instance, *the ECIS calculations for ^{132}Sn(d,p)^{133}Sn are shown in* ***appendix A (Fig.5)***. The angular distributions of the ground state and shell model excited states, corresponding to ΔL transfers ΔL = 1, 3, 5 are given; ΔL = 1,3 are favoured at 5 A.MeV, it is ΔL =3 at 10 A.MeV.

The estimation of the beam intensities are given in the technical document of SPIRAL2 (chap. 2. Performances; yields available on reaction target, after transmission). It will be possible to have beams in the energy domain of 10 A.MeV, by increasing the charge state of the isotopes

extracted from the charge-breeder but the beam intensities will reduced by a factor ~10 compared to those mentioned in the table.
For $^{132-134}$Sn, these yields will still be large enough (> 10^4 pps) to achieve the goals of the (d,p) measurement in a one-week experiment.
By extrapolating these yields we can expect beam intensity for ^{135}Sn around 10^4 pps.
The following table gives the various tin beams available, the Q-value estimated from the mass evaluations [AMDC] and the momentum matching conditions with the calculated ΔL for the various tin beams.

Isotope Ground state J^π	$T_{½}$	intensity (pps) at 5 and 10 A.MeV	Gs	S_n (MeV) [AMDC]	Q[d,p] MeV	ΔL 5 A.MeV	ΔL 10 A.MeV
^{132}Sn 0^+	39.7 s	$> 10^9$ $> 10^7$	$(1h_{11/2})^{12}$	7.31(3)	0.24	2.2	4
133 (7/2-)	1.45 s	$> 10^7$ $> 10^5$	$(f_{7/2})^1$	2.47(4)	1.70	1.8	3
134 0^+	1.12 s	$> 10^6$ $> 10^4$	$(f_{7/2})^2$	3.91(10)	-0.15	2.5	4
135 *	>150ns	$> 10^5$? $> 10^4$?	$(f_{7/2})^3$?	2.07(41)#			

Table 1: Characteristics of the $^{132-135}$Sn isotopes, intensities of the SPIRAL2 beams.

Working at the highest possible incident energies of the SPIRAL2 beams is required, in general, to reach a larger momentum window. The choice of the energies around 10 MeV/n and if possible, higher, is also motivated by the necessity to reduce the straggling in the target, and improve the overall resolution for the measurement of the excitation spectrum.

Experimental conditions

Beam properties

Radioactive beams of interest were given previously. In particular neutron-rich beams of $^{94-98}$Se and $^{94-97}$Kr isotopes, of $^{132-136}$Sn (and neighbours) should be considered.
The minimum intensity required is approximately 10^4 for transfer reactions and 10^5 pps for (p,p') reactions. Preferably, we would like to have as less contaminants as possible in the beam to obtain measurements of transfer and inelastic reactions not dominated by the background events due to reactions induced by the contaminants. A pure beam (more than 90%) is needed to have a clear signature of the direct reactions induced by the beam of interest.
The energy of the beams delivered by CIME (e.g. ~5 *A* MeV for ^{132}Sn in the most probable charge state) are only sufficient for a limited number of transfer studies, i.e. (d, p) and (d, t) transfer reactions with a small angular momentum matching window. Accepting an intensity loss of a factor of ten, the beam energy could be approximately doubled.
The best conditions for the detection (energy losses, straggling, identification) are also obtained using beams at the maximum energies (~10 A.MeV) compatible with the machine and with the needed intensities for our measurements (I>10^4 pps) .

From the technical document on SPIRAL2 facility, it is indicated that energies are ranging from 4.9 to 10 A.MeV. 5-6 A.MeV for ^{132}Sn (q=20+) to ~9-10A.MeV for ^{132}Sn (q=28+). The intensities should be: I=2. 10^9 /s for the 6.0 A.MeV ^{132}Sn beam (charge state q=20+) and 10^8 pps for the 9.4 A.MeV ^{132}Sn beam (q=25+). For the discussion in the LOI we adopted the energies 5 and 10 A.MeV to simplify.

Reaction Targets

For reaction studies using the particle spectroscopy, standard solid targets are the proton-rich CH_2 and deuteron-rich CD_2 solid targets. To minimize the energy and angular straggling, the target thicknesses are typically of the order of 1 mg/cm^2 for CH_2, 0.5 mg/cm^2 for CD_2. Typical energy resolutions obtained with these targets for light exotic beams (A<50) at energy of 10-15 A.MeV are 700 keV FWHM (CH_2 target of 1. mg/cm^2) in (p,p') reactions, and 400 keV (CD_2 target of 0.5 mg/cm^2) in (d,p) reactions; precision which is reached to extract the excitation energies from peak centroids is typically in the range 50-80 keV (for bound states) for the case of unbound states embedded in the continuum the precision is around 200-300 keV and even poorer, as the resonant states have higher excitation energies and have larger widths.

In the case of the SPIRAL2 beams, we want to obtain similar resolutions in excitation energies but the straggling will be an important limitation, especially for the heavier species, and at the lower incident energies of 5 AMeV.

Kinematics

We discuss the kinematics for the ^{134}Sn(d,p) reaction at 10 A.MeV, to illustrate the effect of the mass range on the kinematics and to be used as example of the experimental requirements.

In appendix B the kinematics for the similar reactions, induced by the ^{96}Kr beam on p and d targets are presented, for comparison.

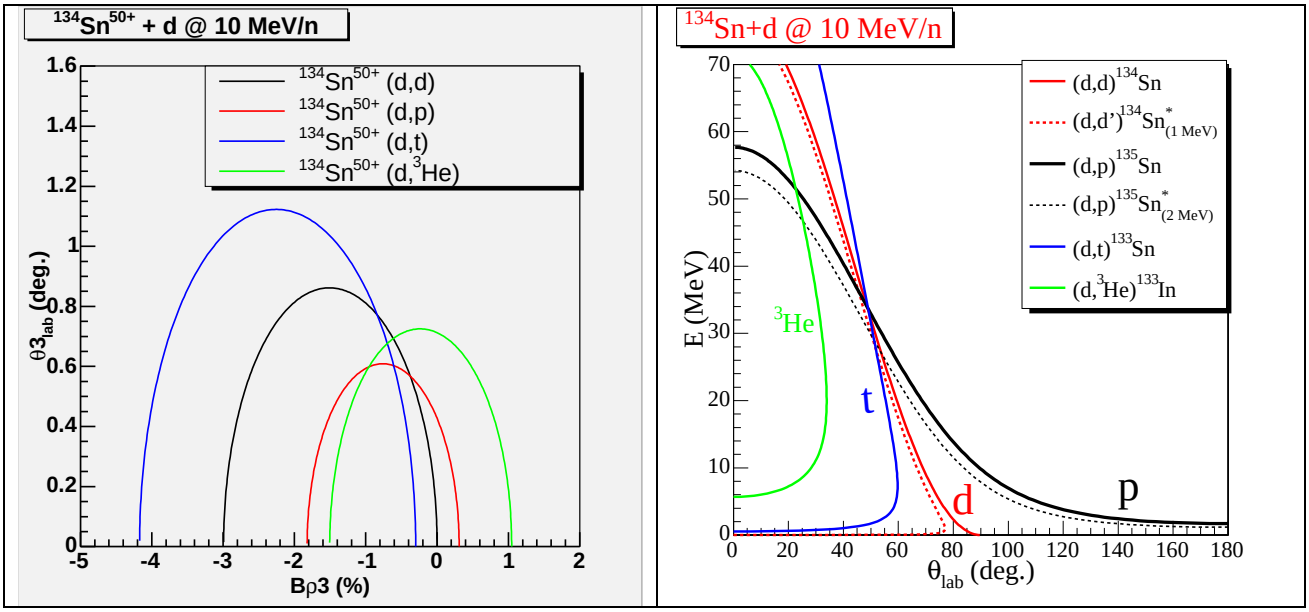

Fig. 4: Kinematics of the particles produced by the reactions ^{134}Sn+d at 10 A.MeV:
- (left) angle (in the laboratory frame) versus variation of the magnetic rigidity for the heavy ejectile detected in the spectrometer,

- (right) energy versus lab. angle of the light charged particles detected in the MUST2 telescope array . The reactions considered here are the (d,p), (d,d'), (d,t) and (d,^{3}He) reactions. They produce p and ^{135}Sn, deuteron and ^{134}Sn, t and ^{132}Sn, ^{3}He and ^{133}In respectively. The counting rates of the (d,^{3}He)In reaction are low (negative Q-value) and the identification of the heavy fragment in coincidence with the light particle will give the signature of the various reaction channels. With reference to the beam direction, the protons will be measured at backward angles from ~100° lab (35° c.m.) to ~160° lab (5° c.m.)*

We see on fig.4 (left) the momentum-angle correlation of the Sn ejectiles for different reactions and the same projectile ^{134}Sn at 10 A.MeV with a CD_2 target: (d,p), elastic scattering on deuteron, and ^{134}Sn(d,t)^{133}Sn (Q = 2.516 MeV). The reaction ^{134}Sn(d,^{3}He)^{133}In (Q = -10.5 MeV) is also indicated. The kinematics of the light ejectiles is given in the right part.
That picture weakly depends on the incident energy, except for the values of the ejectile angles θ_{Sn} in the lab frame, due to the forward focusing of the inverse kinematics.
From the coincidence between light particles and heavy products identified at the focal plane of the spectrometer, it should be possible to separate the various reactions and to measure the transfer (d,p) from 0 to 35° cm. This requires good A&Z identifications; we discuss the identification power in ***Appendix B.***

Experimental set-up in the reaction chamber

The experiment set-up will consist in the coupling between a light charged particle detector and a gamma-spectrometer. The coupling of existing devices, particle telescope and gamma-spectrometer has a low efficiency for the coincident detection of gamma and particle, due to a lack of geometrical overlap.

The full experimental program will be only possible with an improved detection device which integrates the particle and gamma measurements from the design phase; that is GASPARD, as presented in the general LOI "Direct Reaction Studies at SPIRAL2".

Instrumentation and detectors *(equipment to be constructed or modified):*

In the heavy-mass region, nuclei may present high level density of excitation energies. To measure the various reaction channels over a large angular range and record angular cross sections, the gamma-tagging in coincidence with the particle detection will be required, with improved resolution, granularity and efficiency, as compared to the existing array.

On the long-term, to reach the full objectives of the direct reactions program, we will need the **particle-gamma detection array GASPARD (GAmma Spectroscopy and PARticle Detection) and its new design and technique for the combined measurement of particles and gammas.** This equipment will be designed for the detection of proton from 50 keV to 200 MeV and Neon identification from 2 to 1000 MeV. The planned device will offer solid angle coverage close to 4π for both particles and gamma-rays. In such a "4π"+"4π" ensemble, the gamma detectors will surround the particle detectors and be also used to detect the fast charged particles.

GASPARD will include two components: **Particle Array (PA)** and **Gamma Array (GA)**. The PA will be essentially a 4π highly-segmented array surrounding the target. Combined time of flight measurement and Pulse Shape Discrimination will allow the low energy particle

identification. The GA will be also placed in vacuum around the PA. Presently a simple spherical geometry is envisaged.

The main requirements and specifications for the GASPARD-type detection, the technical solutions that are envisaged for the building of a demonstrator, and the estimations of the budget and time schedule of the project can be found in the LOI "Direct Reactions with SPIRAL2".

Beam reconstruction

For the kinematical reconstruction of the reaction and to obtain FWHM energy resolution of, for example, 400 keV (CD_2 target of 0.5 mg/cm^2) in (d,p) reactions, and precision on the measured excitation energies of 100 to 200keV we need to measure the profile and the incident angle of the beam on the target with typical resolutions of 0.5 mm in position and 0.2 deg in angle. This will be done event by event using two beam detectors located upstream the target.

The first generation device used for the GANIL and SPIRAL exotic beams was the CATS. The next-generation detector, adapted to the characteristics of the SPIRAL2 beams (i.e. beams with higher intensity (~10^{7}pps), lower energy (~5 *A* MeV), higher charge (*Z*~50), and consequently with higher energy deposit) is under development. These **Beam Tracking Detectors (BTD**) are presented in **Appendix C.**

Theoretical support *(short description of the necessary calculations and developments):*

Works are in progress to extend the predictive power of the nuclear theories throughout the nuclear chart, to reduce the phenomenological inputs and to establish the foundations of the models on a fully-microscopic basis. From the new developments of the Density functional Theory (DFT) and of its applications within the HFB framework, it is expected that a theory with improved predictive power for the calculations of structure, spectroscopy, and excitations modes will be available for the studies of the intermediate-mass and heavy nuclei.

The theory will include the restoration of broken symmetries, long-range correlations, large amplitude vibrational modes, density-dependent pairing terms deduced from bare *NN* interactions [Dug04]. Such developments are undertaken for instance by T. Duguet and collaborators. In this respect, the data collected on the neutron-rich exotic nuclei could be used as benchmark to test the prescriptions of the new theory.

Other theoretical problems occur when going to the neutron drip-line, along an isotopic chain: the modification of the nuclear forces (spin-orbit, spin-isospin terms) results in a nuclear system which is less and less bound. On the theoretical point of view, the question is not only on the evolution of the nuclear forces with the isospin degree of freedom but also to work in the appropriate framework for the weakly-bound nuclei.

The coupling between bound and continuum states for nuclei close to the drip-line was introduced in HFB calculations [Dob94, Naz94], and several important effects were predicted: increase of pair correlations, of surface diffuseness. Shell gaps are reduced and shell structure is deeply modified by the continuum coupling effects in contrast with the near-stability regions.

Theoretically the description of the exotic nuclei requires the development of the models including the coupling to the continuum and treating explicitly the continuum couplings of bound and scattering states. Such attempts are in progress in the self-consistent mean field model in the HFB approach [Dob96], and also in the shell model framework [Mic02] (Gamow Shell Model GSM) and in the Continuum Shell Model [Vol06].

For instance in [Mic03], the neutron-rich He isotopes are found bound by the Continuum-continuum correlations and the low-lying spectroscopy of the neutron-rich Oxygen isotopes is modified by the continuum coupling (excited states are found at lower energies when the coupling are included).

Analysis of reactions. Our general goal is to learn more about the structure of the nuclei at the driplines, in order to determine the isospin dependence of the effective *NN* interaction.
For reactions involving these weakly-bound nuclei, the scattering states are much closer to the continuum states than in stable nuclei. Consequently, the standard description in terms of well separated bound states from continuum states is no longer valid. To reproduce the data involving light, weakly bound nuclei, such as ^{6}Li [Sak87], ^{6,8}He [Lap01] it was shown that it was necessary to take into account the coupling to the continuum states, favoured by the weak binding energy of these nuclei. These effects are not taken into account in approaches employing optical potentials. The coupling channel effects are playing an important role in the analysis of the direct reactions at low energy [BrS97] and the CDCC calculations for elastic scattering [Sak87,Ska05] were proven to be accurate for the understanding of the nuclear reactions involving weakly-bound nuclei. When going to the drip-lines for neutron-rich nuclei improved theoretical descriptions based upon these coupled channel effects to the continuum will turn out to be crucial to disentangle structure from reaction.
First estimations of the cross sections can be made in a coupled–reaction channel (CRC) framework, using the global parametrizations for the d+nucleus entrance potential [Dae80] and p+nucleus potential [Var91] [Kon93]. Latest developments for the analysis of the one-nucleon transfer reactions [Kee04] include microscopic nucleon-nucleus potentials [JLM77]. They represent a significant improvement for our understanding of the nuclear reactions, and were helpful to analyze the reaction data collected with the ^{8}He SPIRAL beam using the CDCC calculations and the Fresco code [Fresco].
The CRC framework needed for the reaction analysis and the development of new theories coupling structure and reaction are explained in appendix D.
All the developments for structure and reactions are the subjects of the various workshops organized at CEA-Saclay in the virtual laboratory "ESNT" (Espace de Structure Nucléaire Théorique) [ESNT].

APPENDIX A: ESTIMATION OF THE (D,P) CROSS SECTIONS

To illustrate the influence of the incident beam energy we take the example of the ^{132}Sn(d,p)^{133}Sn reaction at 5 and 10A.MeV. The excited states of ^{133}Sn are known.

The estimations of the (d,p) cross sections are obtained in the coupled–channel framework, using the ECIS code [Ray81] and global parametrizations for the d+nucleus entrance potential [Dae80] and nucleon+nucleus potential [Var91] and presented in the figure below.

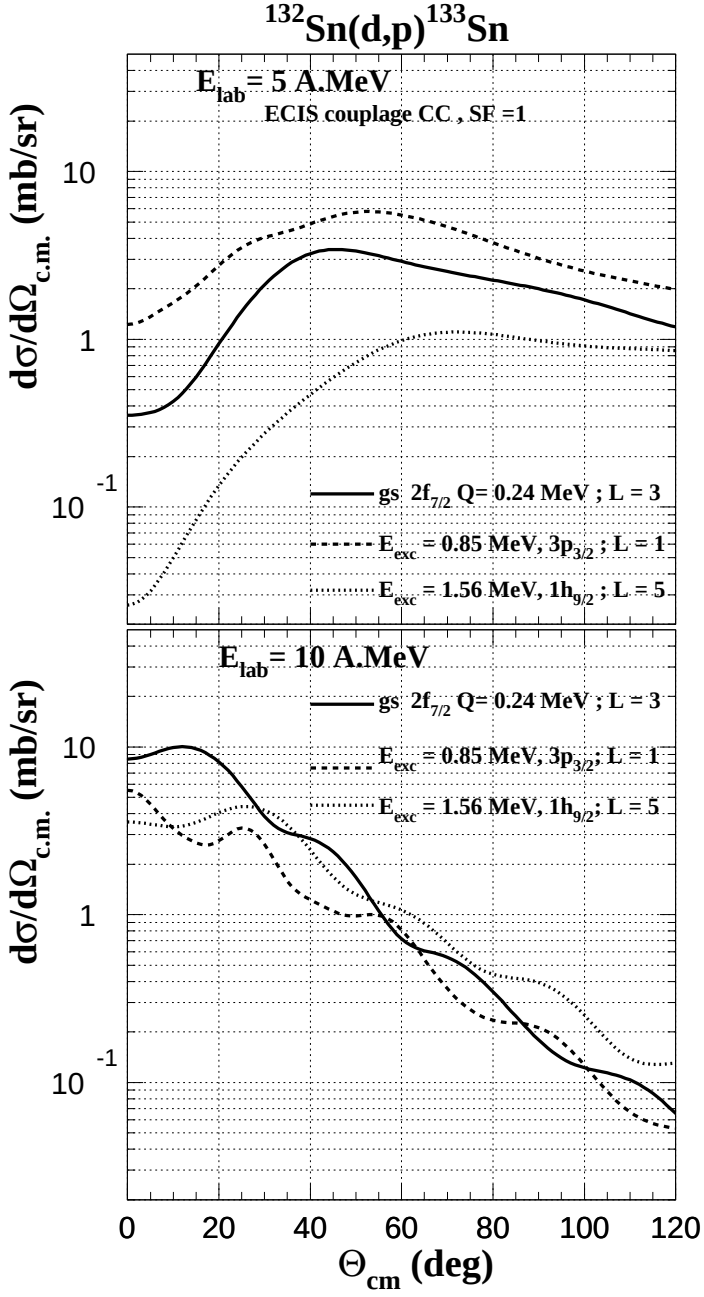

Fig.5: Angular distributions calculated with the ECIS code and global potentials for ^{132}Sn(d,p) ^{133}Sn at 5 and 10 A.MeV.

APPENDIX B: EXPERIMENTAL CONDITIONS

Kinematics of the direct reactions of ^{96}Kr at 10 MeV/n on deuterons and protons.

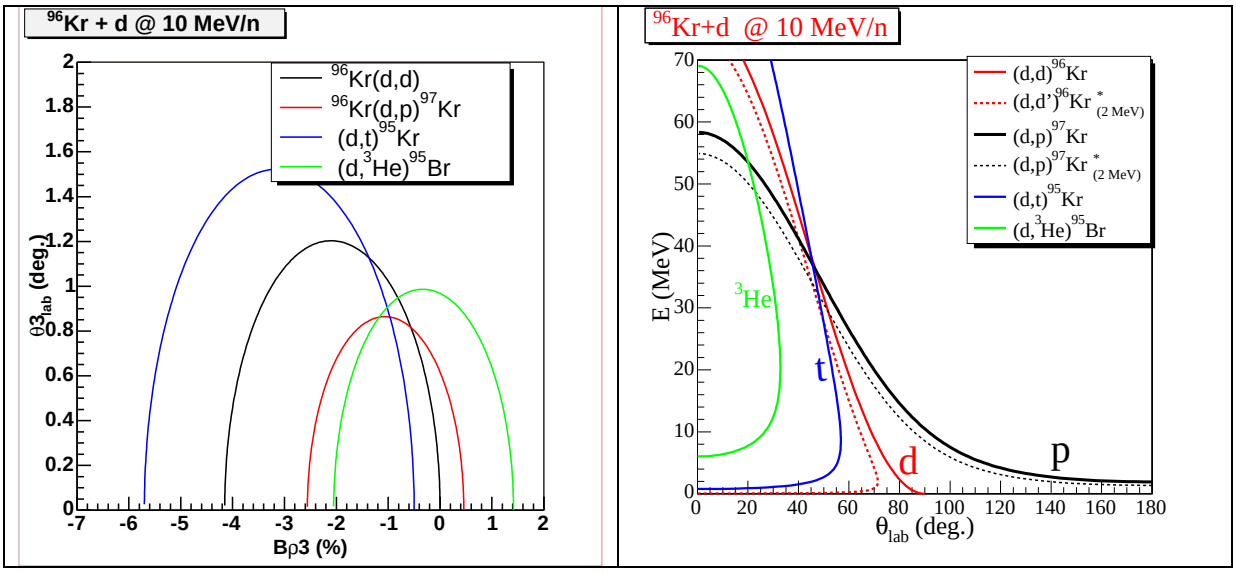

Fig. 6. Kinematics of the ^{96}Kr+d reactions at 10MeV/n for the ejectiles measured at the focal plane of the spectrometer (left) and the light charged particles detected in the MUST2 telescope array (right) (Same axis as Fig. 4). With reference to the beam axis direction, the protons will be measured at backward angles from ~100° lab (35° c.m.) to ~160° lab (5° c.m.)

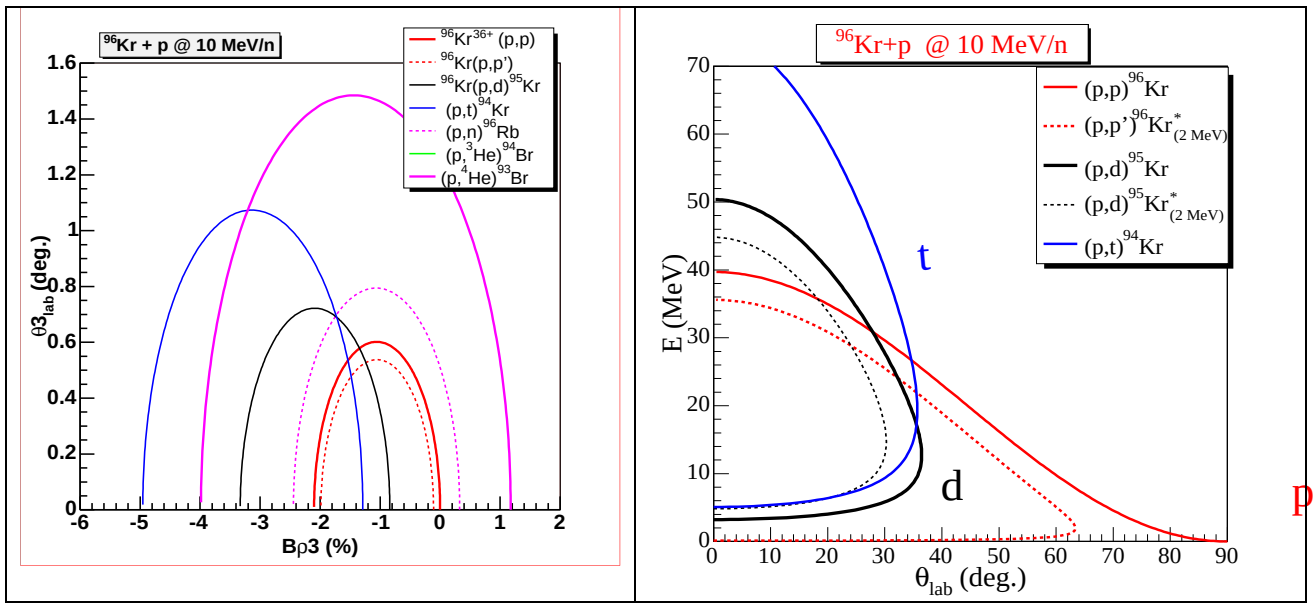

Fig. 7 Kinematics of the ^{96}Kr+p reactions at 10MeV/n for the ejectiles measured at the focal plane of the spectrometer (left) and the light charged particles detected in the MUST2 telescope array (right) . The protons will be measured from ~82° lab (14° c.m.) to ~40° lab

(100° c.m.), and deuterons and tritons will be measured in the angular range from ~10°$_{lab}$ to ~38°$_{lab}$ which corresponds to the c.m. angles from 7°. to 152° for the (p,d) and (p,t).

IDENTIFICATION

We need to measure at the same time other transfer reactions like Sn (d,d'), (d,t). In that case, it is necessary to identify the reaction products. This is currently done after a magnetic spectrometer with a time of flight and energy loss measurement of the particles.

In order to estimate the energy straggling, resolution, identification power etc…, we use the case of the ^{134}Sn(d,p)^{135}Sn, at two incident energies, 5 and 10 A.MeV. These energies correspond to 2 standard energies (different harmonics using CIME cyclotron), which give access to angular momentum window in the spectroscopy of ^{135}Sn (see section on the transfer cross sections).

Energy (A.MeV)	Energy (MeV)	V/c	V(cm/ns)
5	670	0.103	3.10
10	1340	0.145	4.36

Table A.1: parameters of the ^{134}Sn beam.

For the measurement of the (d,p) reaction at the forward c.m. angles (5-35°$_{c.m.}$) corresponding to the proton detected in the backward hemisphere (angles in the lab system from 160°$_{lab}$ down to 100°$_{lab}$), the proton detection is sufficient to have the signature of the (d,p) reaction.
Nevertheless the additional measurement of the heavy ejectile is required:
-first, in order to reduce the background in the excitation spectrum of the ^{135}Sn built from the (d,p) angular yields, using the missing mass method. For instance it will be possible to identify the ^{134}Sn decay product coming from the (d,p) reaction leading to an excited state of ^{135}Sn located above Sn threshold.
-Secondly in order to collect the most complete set of direct reactions (d,p), (d,d), (d,d'), (d,t). These cross sections are needed to provide additional information on the neighbour nuclei, and also to constraint the coupled reaction channel analysis. This is the appropriate framework to extract reliable structure and spectroscopic information. We require the coincidence between the light particle (p, d or t) with heavy ejectile (respectively the ^{135}Sn, ^{134}Sn, ^{133}Sn).
In this mass region, the identification of the ejectile in terms of (A,Z) discrimination, represents an extreme case for the focal plane detection.
[DeltaA =1 over 134, Delta Z=1/50]
To illustrate the identification power required for this experiment we have considered two configurations of the focal plane detection of VAMOS (Drift chambers or SED detectors) and the detection using the SPEG spectrometer. The ejectile which is considered is the ^{134}Sn nucleus with the kinematical characteristics of the incident beam.

Atomic number Z Identification. It requires an energy-loss measurement ΔE combined to either a time of flight t_v or a residual energy E_r measurement. Two values Z_1 and Z_2 may be obtained.

The energy loss will be measured in the ionization chamber [width ~ 50cm C_4H_{10} at 30 Torr] with a resolution $\delta(\Delta E/E)$ assumed to be 3 % and the residual energy E_r in the plastic scintillator with $\delta E_r/E_r$ = 2 %. Z_1 = sqrt(ΔE E) [1]
Since the energy loss in the ionization chamber is large at small incident energy, the total energy has to be considered in (1) instead of E_r and
$(\delta Z_1/Z_1)^2 = [1/2\ (1 + \Delta E/E)\ (\delta(\Delta E)/(\Delta E))]^2 + [1/2\ (E_r/E)\ (\delta E_r/E_r)]^2$ [2]

Energy (MeV)	ΔE (MeV) (io.ch.)	E_r (MeV) Plastics	$\delta Z_1/Z_1$ (%)
670	410.5	259.5	2.45
1340	341.3	998.7	2.03

Table 2 : energy loss in the ionization chamber and deduced Z_1 value.

$$Z_2 = (\text{sqrt}\ \Delta E\}/t_v \quad [3]$$
$$(\delta Z_2/Z_2)^2 = [1/2\ \ (\delta(\Delta E)/(\Delta E))]^2 + [\ (\delta t_v/t_v)]^2 \quad [4]$$

The time of flight t_v may be measured in the two different configurations
- configuration 1 (with drift chambers) between the target and the plastic scintillator over a path equal to l_{path}= 8 meters. We measure the time difference $(t_v)_1=l_{path}/v$ between the RF signal and the scintillator, with a time width $\delta(t_v)_1$ = 2 ns mainly due to the resolution of the RF signal.
- configuration 2 (with SED detectors) between the first SED detector and the plastic scintillator (path equal to 2m). We adopt the same value δt = 0.35 ns for both detectors and $\delta(t_v)_2$ = sqrt{2} * 0.35 = 0.5 ns.
Assuming that Z_1 and Z_2 are two independent measurements of the atomic number, the final resolution on Z is improved due to

$$1/[\delta Z/Z]^2 = 1/[\delta Z_1/Z_1]^2 + 1/[\delta Z_2/Z_2]^2 \quad [5]$$

Energy (A.MeV)	v (cm/ns)	$(t_v)_1$ 8m	$\delta t_{v1}/t_{v1}$ (%)	$\delta Z_1/Z_1$ (%)	$\delta Z_2/Z_2$ (%)	$\delta Z/Z$ (%)
5	3.10	259.	0.77	2.5	1.7	1.4
10	4.36	184.	0.15	2.0	1.8	1.4

Table A3: configuration 1 (drift chambers).

Since from Drift to SED configurations the time resolution evolves from 2 to 0.5 ns (factor ¼) and the path is also divided by ¼, $\delta(t_v)_2/(t_v)_2 = \delta(t_v)_1/(t_v)_1$ and the corresponding $\delta Z_2/Z_2$ and $\delta Z/Z$ are equal for both configurations.
Since we deal with Z = 50 the needed resolution is 2 % FWHM to discriminate between Z and Z ±1, which corresponds to the minimum Z resolution equal to 1 % (sigma). That value will not be obtained. It is very dependent on the energy loss resolution of the ionization chamber which was assumed to be 3%, but also on the time resolution.

If the experiment was done with the SPEG spectrometer, the path between the target and the plastic scintillator, equal to 14m, would result in the improvement of $\delta t_{v1}/t_{v1}$ in the

configuration 1. This corresponds to the improvement of δZ/Z to 1.3% (see table A4) still limited by the resolution of the energy loss measurement.

Energy (A.MeV)	v (cm/ns)	$(t_v)_1$ 14m	$\delta t_{v1}/t_{v1}$ (%)	$\delta Z_1/Z_1$ (%)	$\delta Z_2/Z_2$ (%)	$\delta Z/Z$ (%)
5	3.10	453.	0.4	2.5	1.6	1.3
10	4.36	321.	0.6	2.0	1.6	1.3

Table A4: configuration 1 (drift chambers) with the SPEG spectrometer.

Mass Identification. The mass number A is obtained from again two independent measurements.
From the position measurement in the focal plane, we obtain the magnetic rigidity Bρ. Combined to the time of flight t_v, the ratio mass over charge (A/q) is obtained. However, the charge state q has to be determined exactly. A_1/q proportional to B ρ t_v [6]

$$\text{and } [\delta(A_1/q)/(A_1/q)]^2 = (\delta(B\rho)/(B\rho))^2 + (\delta t_v/t_v)^2 \quad [7]$$

With A = 132, we have 0.8 % between A and A ± 1, which implies a mass resolution better than 0.4 % (sigma). It is clearly seen from table A3 that the time resolution has to be improved by at least a factor of 2. That means an improvement of the time signals, an increase of the path, or both. Assuming the nominal value $\delta(B\rho)/(B\rho) = 0.1$ %, we get

Energy (A.MeV)	$(t_v)_1$ (ns)	$\delta(t_v)_1/(t_v)_1$ (%)	$\delta A_2/A_2$ (%)	$\delta(A_1/q)/(A_1/q)$ (%)
5 VAMOS	259.	0.8	3.9	0.8
5 SPEG	453.	0.4	3.7	0.5
10	184.	1.1	4.2	1.1

Table A5: configuration 1 (drift chambers).

With the total energy E and the time of flight t_v, we deduce the mass from
the usual kinematical relation A_2 proportional $E\,(t_v)^2$ [8]
and $(\delta A_2/A_2)^2 = (\delta E/E)^2 + (2\delta t_v/t_v)^2$ [9]

The total energy is calculated as the sum $\Delta E + E_r$. If we may neglect the energy straggling introduced by the target and the different plastic foils, we have δE/E = 3.6 %. With the time resolution taken into account, we obtain the mass resolution $\delta A_2/A_2$.
That mass resolution is not good enough, but it does not depend on the unknown charge state q. If we reintroduce that A_2 value in (6), we will obtain the charge state q with the same resolution $\delta q/q = \delta A_2/A_2$. With the values quoted in Tables A4 and 5, the charge state q will be clearly identified up to q ~ 12. Then, it may be reintroduced in (6) with its integer value and A_1 will be known with the resolution δ (A/q) / (A/q) quoted in Table 5.
For larger values of the charge state, q ≥12, only the ratio A_1/q will be known with that resolution, and the mass A_1 will not be completely resolved.

The larger path in the SPEG spectrometer may be an advantage, especially for heavy beams like the Tin isotopes around ^{132}Sn. In that case, due to the strong forward focusing; all the ejectiles are emitted in a narrow cone, compatible with the small angular coverage of SPEG, +/- 2 deg in both horizontal and vertical planes.

Note that for the nuclei with lower A, Z numbers (A < 100, Z < 40) the 2 configurations of the detection will be enough to achieve a sufficient identification.
It means that the direct reactions in the region of the neutron-rich Kr isotopes, will be performed without further development of the detection, simply by combining detectors similar to MUST2, VAMOS and EXOGAM (to separate gamma-rays for nuclei of interest).
For the heavier nuclei, a focal plane detection similar to the one of SPEG (larger flight path than the one of VAMOS), and a modification of the ionization chamber to improve the resolution will be required.

APPENDIX C: INSTRUMENTATION

Beam Tracking Detectors Radioactive-ion beams available today often have a large emittance and beam tracking devices (BTD) are then needed to perform precision experiments. In 2004-05 we have worked on the development of BTDs for SPIRAL beams. While the current beam tracking detectors have been optimized for relatively light ion beams, a further optimization is required for a use with SPIRAL2 beams, i.e. beams with higher intensity (~10^7pps), lower energy (~5 *A* MeV), higher charge (*Z*~50), and consequently with higher energy deposit.
Minimum rates of the SPIRAL2 beams are ranging from a few hundred to a few 10^4 pps. For rates higher than 10^6 pps, the beam tracking becomes no longer possible and additional specifications are necessary. The beam emittance must be low in order to allow sufficient angular resolution which, in turn, affects the resolution of the reconstructed excitation energy. Finally, the RF signal should have sufficient resolution, better than 1 ns, to allow the identification of recoil particle in the energy domain where the E-TOF technique is used. Pulse shape discrimination is important when the RF time resolution is poor.
The system requires a development of a Beam Tracking Detector (BTD) that will give the position on target with a resolution of 0.5 mm and an angular resolution of 0.2°. The device should have a time resolution below 0.5 ns for ions heavier than Ne. What is crucial with the BTD for SPIRAL2 beams is to have a small mass interception. The SPIRAL2 beams will be medium-mass ions with high charge. The thickness of the material intercepting the beam has to be below 50µg/cm^2 of equivalent carbon foils. In May 2005, the scientific and technical council of the SPhN division has given a positive response to the BTD program to be undertaken by DAPNIA/SPhN and SEDI. Results of the R&D are expected within 2 years.
R&D should include:

i) Intensive work to optimise low-pressure gas detectors.
ii) Further studies of the present detector configurations.
iii) Study of new original configurations (Micromegas, diamond detectors…)
iv) Study of fast electronics and high-rate sampling for time resolution (MATACQ).

The BTD project has involved around 3 men-years, including engineers and technicians from SEDI. The collaboration involves DAPNIA, GANIL, IPN-Orsay, SPhN, and the project leader is A. Drouart (SPhN). Project status: 1st stage achieved, preliminary design for 2nd stage, further R&D needed; Project costs: 40 kEuros (2006-07).
Engineering time estimate: 3 years (engineers and technicians from SEDI).

APPENDIX D
DEVELOPMENTS IN STRUCTURE AND REACTIONS THEORIES

The Distorted Wave Born Approximation was the source of powerful nuclear studies, but generally speaking, possible coupling of the elastic scattering to the inelastic or other reaction channels might occur and modify deeply the reactions features [Sat78,Sat83]. Theories beyond the DWBA [Sat78] are required if we want to analyze our reaction data and be able to understand the features of elastic, inelastic and transfer reaction data in a consistent way. For instance, the DWBA was shown to be "inappropriate for the analysis of (d, p) reactions some 30 years ago, due to the importance of the deuteron breakup channel" [Tim99], the appropriate framework was the adiabatic approach from Johnson & Soper including explicitly the deuteron break-up [Tim99]. Through the CDCC calculations, it is possible to take into account the continuum coupling and break-up effects in reactions involving a loosely bound nucleus. The new developments of CDCC, with the eXtended Continuum Discretized Coupled Channel (XCDCC) method, provide the framework to describe the core transitions in the breakup of exotic nuclei [Sum06].
Theoretical developments in the line of SMEC (shell model embedded in the continuum) [Ben99] are foreseen to build reaction-structure models and to incorporate in the reaction analysis the complete treatment of the continuum couplings. Improved description of the particles embedded in the continuum during a transfer reaction will be needed.

Since we will work with weakly-bound nuclei and perform reactions at low energies, we can expect the coupled reaction-channel effects to be of importance in our analysis, as shown by our previous works with the SPIRAL beams. They have revealed the importance of taking into account the couplings between the main reaction channels (elastic and inelastic scattering, 1n and 2n transfer reactions) in the theoretical analysis.
At low energy roughly below 20 MeV/n, the relative counting rates of the elastic, inelastic scattering, 1n and 2n transfer are deeply modified from our usual understanding of these processes and this phenomenon is even more pronounced for a weekly-bound nucleus like ^{8}He, loosing more easily nucleons (S_n =2.5 MeV, S_{2n} =2.1 MeV) than getting excited (E_{exc} = 3.6 MeV). We showed that the analysis of these reactions involving a weakly-bound nucleus requires a coupled-channel analysis [Ska05,Ska06].
The influence of the one-nucleon transfer reaction on the elastic and inelastic process crucially depends on the spectroscopic factor : for instance in the ^{A}Z(p,d) $^{A-1}$Z reaction, the larger the SF between $^{A-1}$Z and ^{A}Z, the higher the cross sections of the (p,d) compared to the elastic ones. The coupled channel effects are also more pronounced at low incident energies. It means that the commonly used DWBA framework is no longer valid, *a priori*, to analyze the direct reactions which are scheduled in this experimental program.
The effects of such couplings are enhanced at low incident energies (typically below 20 A.MeV) and, for reactions involving weakly-bound nuclei. They are *a priori* significant and must be controlled.
The analysis of a given reaction will not provide unambiguously the structure data. To extract a reliable structure information, several reactions will be studied, and their correlations. This means:

i) That a coupled reaction framework analysis is needed to understand the measured reactions,

ii) That a complete measurement of the main reaction yields is needed. In particular, we will measure elastic and inelastic scattering (d,d') (p,p') to estimate excitation and coupling effects and determine the appropriate proton –nucleus and deuteron-nucleus optical potentials.

REFERENCES

[AMDC] Mass Evaluation: A. Wapstra, G. Audi and C. Thibault, NP*A729*, 129 (2003).
and http://www-csnsm.in2p3.fr/amdc/web/masstab.html
[Adr95] P. Adrich *et al.*, Phys. Rev. Lett. **95**, 132501 (2005).
[Ben99] K. Bennaceur *et al.*, Nucl. Phys. **A651**, 289 (1999); **A671**, 203 (2000); Phys. Lett. B **488**, 75 (2000).
K. Bennaceur, J. Dobaczewski, M. Ploszajczak, Phys. Rev. C **60,** 034308 (1999).
[Bec06] E. Becheva *et al.*, Phys. Rev. Lett. 96, 012501 (2006).
[Bjo86] T. Bjørnstad *et al.*, Nucl. Phys. **A453**, 463 (1986).
[Bla02] J. Blachot, Nucl. Data Sheets **97**, 593 (2002).
[BrS97] M.E. Brandan and G. R. Satchler, Phys. Rep. 285, 143 (1997).
[CATS] S. Ottini *et al.*, NIM A 431 (1999) 476.
[Cha95] E.Chabanat, P.Bonche, P.Haensel, J.Meyer, R.Schaeffer, Phys.Scr. T56, 231 (1995).
[Cha97] E.Chabanat, P.Bonche, P.Haensel, J.Meyer, R.Schaeffer, Nucl.Phys. **A627**, 710 (1997).
[ChW92] W.-T.Chou, E.K.Warburton, Phys.Rev. C**45**, 1720 (1992).
[Dae80] W. W. Daehnick *et al.*, Phys. Rev. C **21** 2253 (1980).
[Dea04] D. J. Dean,T. Engeland, M. Hjorth-Jensen, M. P. Kartamyshev, E. Osnes, Prog. Part. Nucl. Phys. 53, 419 (2004).
[Dec80] J. Dechargé and D. Gogny, Phys. Rev. C **21**, 1568 (1980).
[Dob94] J. Dobaczewski et al., Phys. Rev. Lett. **72**, 981 (1994).
[Dob95] J. Dobaczewski, W. Nazarewicz, T.R. Werner, Physica Scripta T56 (1995) 15.
[Dob96] J. Dobaczewski, W. Nazarewicz, T.R. Werner, J.F. Berger, C.R. Chinn, J. Dechargé, Phys. Rev. C **53,** 2809 (1996).
[Dug04] T. Duguet, Phys. Rev. C **69**, 054317 (2004).
[ESNT] information (programs, contents) on the various theory workshops is available on the web site of SPhN, http://www-dapnia.cea.fr/Sphn/ (on the left part of the menu, click on "Espace de Structure Nucléaire Théorique")
[Fog95] B. Fogelberg, *et al.*, Phys. Rev. Lett. **73**, 2413 (1994).
[Fresco] I. J. Thompson, Fresco code, Comput. Phys. Rep. **7** (1988) 167.
[Gau06] L. Gaudefroy *et al.*, Phys. Rev. Lett. **97**, 092501 (2006).
[JLM77] J.-P. Jeukenne, A. Lejeune, and C. Mahaux, Phys.Rev. C **16** (1977) 80.
[Jou05] C. Jouanne, V.Lapoux et al., PRC **72**, 014308 (2005).
[Kee04] N. Keeley, N. Alamanos, and V. Lapoux, Phys. Rev C **69**, 064604 (2004)
[Kon03] A.J. Koning and J.P. Delaroche, Nucl. Phys.*A713* (2003) 231.
[Lag01] A. Lagoyannis *et al.*, Phys. Lett. B **518,** 27 (2001).
[Lal05] G. A. Lalazissis,T. Niksic, D.Vretenar, and P. Ring, Phys. Rev. C **71**, 024312 (2005).
[Lap01] V. Lapoux *et al.*, Phys. Lett. B **517**, 18 (2001).
[Mic02] N. Michel *et al.*, Phys. Rev. Lett. **89,** 042502 (2002).

[Mic03] N. Michel, W. Nazarewicz, M. Ploszajczak and J. Okolowicz, Phys. Rev. C **67,** 054311 (2003).
[MUST] Y. Blumenfeld *et al.,* The MUST collaboration, NIM **A 421** (1999) 471-491.
[MUST2] E.C. Pollacco *et al.,* The MUST2 collaboration, EPJA **25**, 287 (2005) .
[Naz94] W. Nazarewicz et al., Phys. Rev. C **50**, 2860 (1994).
[Obe05] A. Obertelli, S. Péru, J.-P.Delaroche, A.Gillibert, M. Girod, and H. Goutte, Phys.Rev. C **71**, 024304 (2005).
[Obe06] A. Obertelli *et al.,* Phys. Lett B **633**, 33 (2006).
[Omt95] J.P. Omtvedt *et al.,* Phys. Rev. Lett. **75**, 3090 (1995).
[Oza00] A. Ozawa *et al.*, Phys. Rev. Lett. **84**, 5493 (2000).
[Ots01] T. Otsuka *et al.*, Phys. Rev. Lett. **87**, 082502 (2001).
[Ots03] T. Otsuka *et al.*, Phys. Rev. Lett. **91**, 179202 (2003).
[Ots05] T. Otsuka *et al.*, Phys. Rev. Lett. **95**, 232502 (2005).
[Paa03] N. Paar, P. Ring, T. Niksic and D. Vretenar, Phys. Rev. C **67**, 34312 (2003).
[Ray81] J. Raynal, Phys. Rev. C **23**, 2571 (1981).
[Sak87] Y. Sakuragi, Phys. Rev C **35**, 2161 (1987).
[Sat78] R. Satchler, Review of Modern Physics, Vol 50, No.1, Part1., Jan. 1978.
[Sat83] R. Satchler, Ed. Clarendon Press, Oxford Univ Press 1983.
[Ska05] F. Skaza et al., Phys. Lett. B **619,** 82 (2005).
[Ska06] F. Skaza *et al*., Phys. Rev. C **73**, 044301 (2006)
[Sta04] M.Stanoiu *et al.,* Phys. Rev C **69**, 034312 (2004).
[Sto03] M.V. Stoitsov, J. Dobaczewski, W. Nazarewicz, S. Pittel and D.J. Dean, Phys. Rev. C**68**, 054312 (2003).
[Sum06] N. C. Summers, F. M. Nunes, and I. J. Thompson, Phys. Rev. C **73**, 031603 (2006).
[Ter02] J.Terasaki, J.Engel, W.Nazarewicz, M.Stoitsov, Phys.Rev. C 66, 054313 (2002).
[Tim99] N. Timofeyuk and RC Johnson, Phys. Rev C **59**, 1545 (1999).
[Tod04] B. G. Todd-Rutel *et al.*, Phys. Rev. C **69**, 021301(R) (2004).
[Var91] R.L. Varner, W.J Thompson, T.L. McAbee, E.J. Ludwing and T.B Clegg, Phys. Rep. **201** (1991) 57.
[Vol06] A. Volya and V. Zelevinsky, Phys. Rev. Lett. **94**, 052501 (2005).
[Wil69] B.H. Wildenthal, Phys. Rev. Lett. **22**, 1118 (1969); B.H. Wildenthal and Duane Larson, Phys. Lett. B**37**, 266 (1971).